Model for the simulation of swelling-pressure measurements on expansive soils

Fangsheng Shuai and D.G. Fredlund

Abstract: Numerous laboratory swelling tests have been reported for the measurement of swelling pressure and the amount of swell of an expansive soil. These test methods generally involve the use of a conventional one-dimensional oedometer apparatus. Few attempts, however, have been made to formulate a theoretical framework to simulate the testing procedures or to visualize the different stress paths followed when using the various methods. The simulation of the oedometer tests on expansive soils is required to fully understand the prediction of heave. The correct measurement of swelling pressure is required for an accurate prediction of heave. It is further anticipated that some information on unsaturated soils property functions may be approximated from the back-analysis of the data. A theoretical model is proposed to describe the pore-water pressures with time and depth in a specimen as well as the volume changes during various oedometer swell tests. The model is formulated based on equilibrium considerations, constitutive equations for an unsaturated soil, and the continuity requirement for the pore fluid phases. The transient water flow process is coupled with the soil volume change process. The model can be used to describe the volume-change behaviour, pore-water pressure, and vertical total stress development in an unsaturated soil during an oedometer test performed by any one of several test procedures. The model has been put into a finite element formulation using the Galerkin technique. All the parameters required to run the model can be obtained by performing independent, common laboratory tests. The proposed model was used to simulate the results from free-swell, constant-volume, constant water content, and loaded-swell oedometer tests. Computed values of volume change, vertical total stress, and pore-water pressure are in good agreement with measured values.

Key words: unsaturated soil, expansive soil, swelling pressure, theoretical simulation, constant-volume oedometer test, free-swell oedometer test, loaded-swell oedometer test.

Résumé : On a déjà mentionné de nombreux essais de gonflement en laboratoire pour mesurer la pression et l'amplitude de l'expansion d'un sol gonflant. Ces méthodes d'essai impliquent généralement l'utilisation d'un appareil oedométrique uni-dimensionnel classique. On trouve pourtant peu de tentatives faites pour formuler un cadre théorique simulant les procédures d'essai ou pour visualiser les différents chemins de contrainte suivis au cours des diverses méthodes. La simulation des essais oedométriques sur des sols gonflants est nécessaire pour une prédiction bien comprise du soulèvement. La mesure correcte de la pression de gonflement est indispensable pour évaluer le soulèvement avec précision. On s'attend également à tirer de l'analyse à rebours des résultats quelque information, même approximative, sur les fonctions propres aux sols non saturés. On propose ici un modèle théorique pour décrire les pressions interstitielles au cours du temps et sur toute l'épaisseur de l'échantillon ainsi que les changements de volume pendant divers essais de gonflement oedométriques. Le modèle est basé sur des considérations d'équilibre, des équations constitutives pour un sol non saturé et une condition de continuité de la phase interstitielle. Le processus d'écoulement hydraulique transitoire est couplé avec le processus de changement de volume du sol. Le modèle peut être utilisé pour décrire le comportement en changement de volume et en pression interstitielle. On peut aussi suivre le développement de la contrainte verticale totale dans un sol non saturé pendant un essai oedométrique suivant une méthode au choix. Le modèle a été introduit dans une formulation par éléments finis utilisant la technique de Galerkin. Tous les paramètres nécessaires à l'exécution du modèle peuvent être obtenus lors d'essais de laboratoire indépendants et classiques. Le modèle proposé a été utilisé pour simuler les résultats d'essais oedométriques du type gonflement libre, à volume constant, à teneur en eau constante et à gonflement sous charge. Les valeurs calculées pour le changement de volume, la contrainte verticale totale et la pression interstitielle sont en bon accord avec les valeurs mesurées.

Mots clés : sols non saturés, sols gonflants, pression de gonflement, simulation théorique, essai oedométrique à volume constant, essai oedométrique à gonflement libre, essai oedométrique à gonflement sous charge.
[Traduit par la rédaction]

Introduction

Expansive soils are found in many parts of the world, particularly in semiarid regions. Expansive soils are generally unsaturated and contain clay minerals that exhibit high volume change upon wetting. Under confined conditions, expansive

Received June 10, 1997. Accepted September 2, 1997.

F. Shuai and D. G. Fredlund. Department of Civil Engineering, 57 Campus Drive, University of Saskatchewan, Saskatoon, SK S7N 5A9, Canada.

soil will exhibit considerable swelling pressures which result in serious damage to buildings and other structures. Lightly loaded structures, such as roadways, airport runways, or small buildings, which are built on expansive soil are often subjected to serious cracking and distress, even distortion of the frame structure, subsequent to construction due to the changes in the surrounding environment. Krohn and Slosson (1980) estimated that, in the United States alone, the money spent on damage caused by expansive soil amounts to about $7 billion per year. Jones and Holtz (1973) pointed out that the damage due to swelling soils is more than twice that of the combined damages from natural disasters such as floods, hurricanes, earthquakes, and tornadoes. As a result of the costs involved, problems associated with expansive soils have attracted wide attention around the world.

Numerous procedures have been proposed to measure the swelling pressure and to predict the amount of heave in different parts of the world. The swelling pressure becomes the indicator of the present state of stress in the soil and plays an integral part in the prediction of heave. These methods generally involve the use of a one-dimensional oedometer apparatus. The free-swell, constant-volume, and loaded-swell tests are among the most commonly used procedures. A large number of laboratory tests and practical experience have been assimilated involving these methods. In contrast, little attempt has been made to formulate a theoretical framework to simulate these testing procedures and to visualize the different stress paths used in the various methods. A theoretical model is vital in the interpretation of the one-dimensional oedometer test data.

It is well known that measured swelling pressures and predicted heaves differ significantly depending on the test procedure used to measure the expansive soil properties (Brackley 1975; Ali and Elturabi 1984; Sridharan et al. 1986). From a practical application perspective it is difficult to say which test procedure is most suitable without fully understanding the stress paths followed during the different testing procedures.

The objective of this research program is to formulate a theoretical framework which can embrace all of the laboratory swelling test procedures. The proposed theoretical framework can accommodate various boundary conditions and help to visualize the stress paths followed by each of the procedures. The study is mainly limited to one-dimensional swelling under various oedometer testing conditions.

Testing procedures for the measurement of swelling pressure in expansive soil

The one-dimensional consolidation apparatus (i.e., oedometer) has become widely used for testing swelling soils. Holtz and Gibbs (1956), Jennings and Knight (1957), and Lambe and Whitman (1959) were among the first to report the use of oedometer tests for predicting heave in swelling soils. The more commonly used testing procedures for determining the swelling pressure of a soil can be described as (*i*) free swell under a token load followed by compression (i.e., free-swell oedometer test), (*ii*) different surcharge loadings followed by inundation (i.e., loaded-swell oedometer test), and (*iii*) constant-volume loading followed by rebound (i.e., constant-volume oedometer test). These commonly used oedometer test procedures can be further subdivided into two broad categories, namely swell under constant load (constant-load oedometer test) and swell under constant volume (constant-volume oedometer test). The first category involves tests where a constant applied load is maintained during inundation of the specimen (i.e., free-swell or loaded-swell oedometer test). The second category involves tests which permit a change in the applied load under no change in volume (i.e., constant-volume oedometer test).

In the free-swell oedometer test, the soil specimen is brought in contact with water and allowed to swell freely with a token load applied. Then the soil is gradually consolidated back to its original volume in the conventional manner of a consolidation test procedure (Fig. 1*a*). The swelling pressure

Fig. 1. Stress path representation for the free-swell oedometer test (from Fredlund 1995). (*a*) Conventional free-swell data plot. (*b*) Three-dimensional stress-path plot. e_0, initial void ratio; w, water content; w_o, initial water content; G_s, specific gravity of solids.

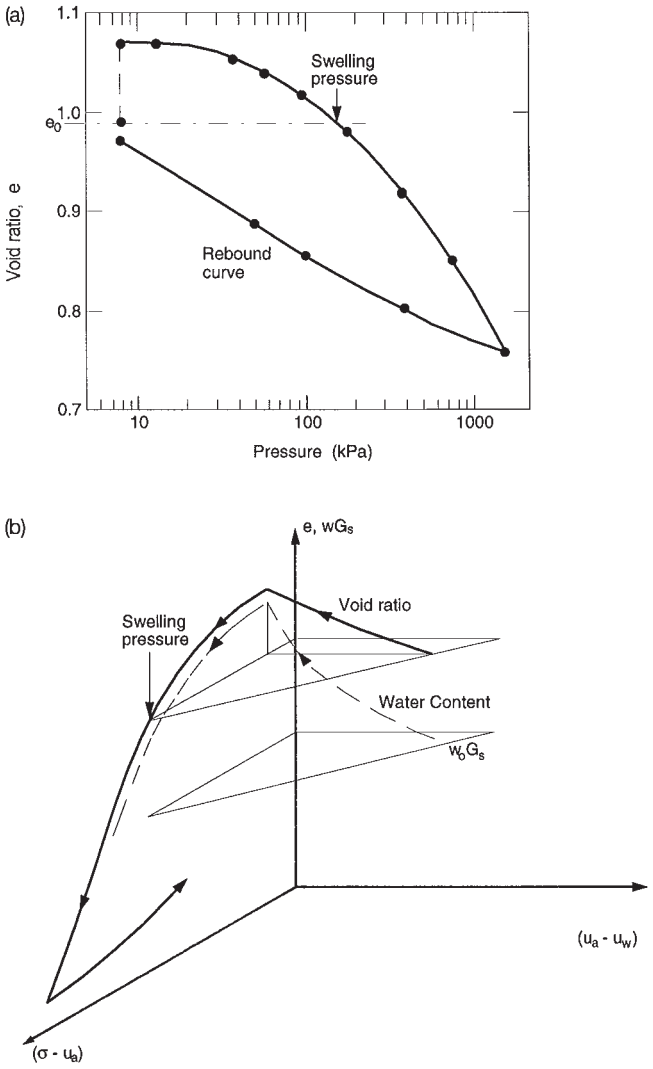

Fig. 2. Stress path followed in the loaded-swell test. (*a*) Two-dimensional plot. (*b*) Three-dimensional plot.

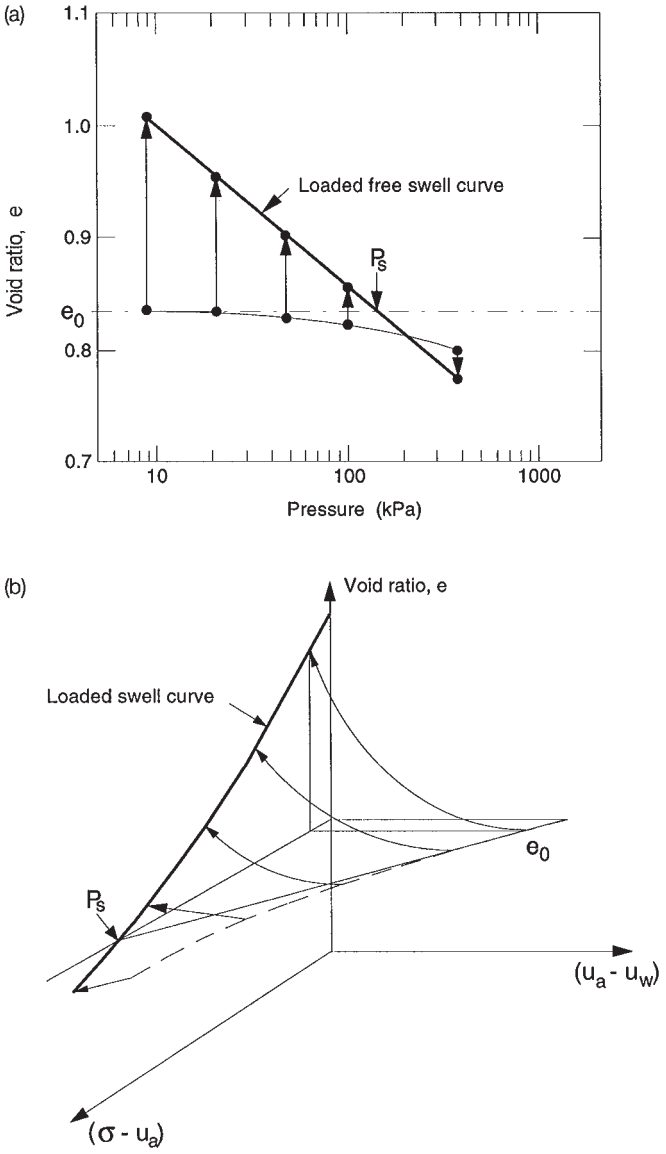

Fig. 3. Stress path followed in the constant-volume oedometer test (from Fredlund 1995). (*a*) Conventional constant-volume data plot. (*b*) Three-dimensional stress-path plot.

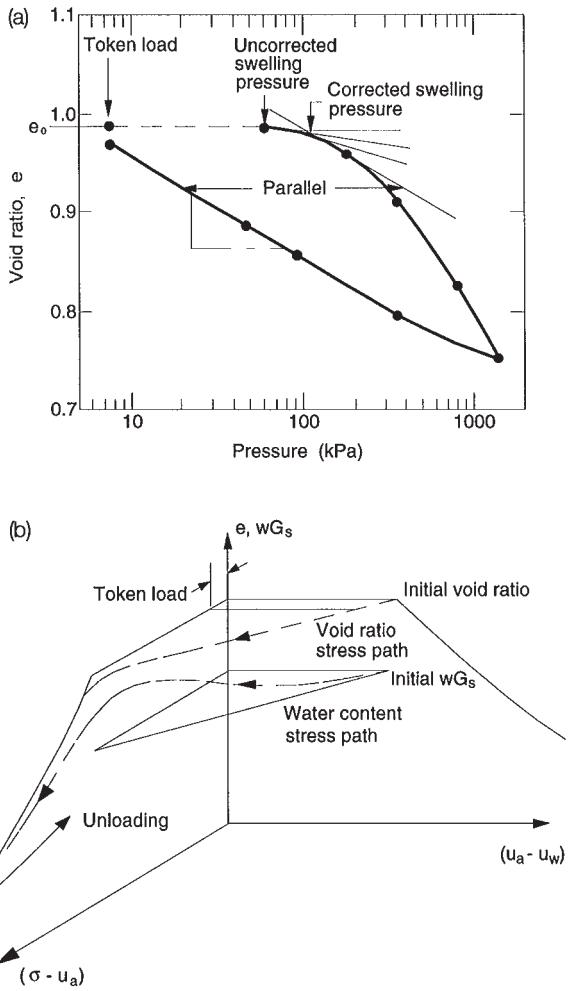

is defined as the stress necessary to consolidate the specimen back to its original volume (Hardy 1965; Sridharan et al. 1986). The stress paths adhered to can be more clearly understood using a three-dimensional plot with the stress state variables $(\sigma - u_a)$ and $(u_a - u_w)$ forming the abscissas (Fig. 1*b*), where σ is the total normal stress, u_a is the pore-air pressure, and u_w is the pore-water pressure.

In the loaded-swell oedometer test, a number of "identical" specimens are subjected to different initial applied loads and allowed to swell freely. The resulting final volume changes are plotted against the corresponding applied loads or stresses. The stress corresponding to zero volume change is termed the swelling pressure (Skempton 1961; Gizienski and Lee 1965; Nobel 1966; Matyas 1969). The stress path for the loaded-swell tests is shown in Fig. 2.

In the constant-volume test procedure, a specimen is subjected to a token load and immersed in water. The specimen volume is maintained constant throughout the first part of the test by varying the load applied to the specimen as required. This procedure is continued until there is no further tendency for swelling. The applied load at this point is referred to as the "uncorrected" swelling pressure, P_s (Fredlund et al. 1980). The soil specimen is then further loaded and unloaded following the conventional oedometer test procedure. The test results are commonly plotted as shown in Fig. 3*a*. The actual stress paths followed during the test can be visualized using a three-dimensional plot of the stress state variables versus void ratio or water content (Fig. 3*b*). To empirically account for sampling disturbance, Fredlund et al. (1980) defined a correction procedure which could be applied to the data to give a "corrected" swelling pressure. The correction procedure is a

modification of the Casagrande type of geometrical construction as shown in Fig. 3.

General theory

Swelling oedometer tests primarily involve two processes, namely the transient water flow process and the soil volume change process. These two processes are linked with each other and governed by the following basic equations: (*i*) the force equilibrium equation for an element of soil, (*ii*) the constitutive equations for unsaturated soils, and (*iii*) the continuity equation for the pore fluids.

Force equilibrium

For the one-dimensional case, the force equilibrium equation can be written in an incremental form as follows:

$$[1] \qquad \frac{\partial \Delta\sigma_z}{\partial z} = 0$$

where $\Delta\sigma_z$ is the increment of total normal stress with time in the z direction (i.e., $\Delta\sigma_z = \sigma_z(t = t_1) - \sigma_z(t = 0)$).

Volume change constitutive relationships

Fredlund (1979) proposed volume change constitutive relationships for an unsaturated soil as an extension of the form of equation used for a saturated soil, using the net normal stress ($\sigma_z - u_a$) and matric suction ($u_a - u_w$) as the stress state variables. For a one-dimensional case, the relationship for the soil structure can be written as

$$[2] \qquad \varepsilon_z = \frac{\Delta V_v}{V_0} = m_1^s \Delta(\sigma_z - u_a) + m_2^s \Delta(u_a - u_w)$$

The following constitutive relationship can be written for the water phase:

$$[3] \qquad \frac{\Delta V_w}{V_0} = m_1^w \Delta(\sigma_z - u_a) + m_2^w \Delta(u_a - u_w)$$

where

Δ is the increment of the stress states with time;
ε_z is the the strain in the z direction;
σ_z is the total normal stress in the z direction;
V_0 is the initial overall volume of the soil element;
ΔV_v is the change in the volume of soil voids in the soil element;
$m_1^s = [(1 + \mu)(1 - 2\mu)]/[E(1 - \mu)]$, the soil structure volume change modulus with respect to a change in net normal stress;
$m_1^s = (1 + \mu)/[H(1 - \mu)]$, the soil structure volume change modulus with respect to a change in matric suction;
E is the modulus of elasticity or Young's modulus for the soil structure;
μ is Poisson's ratio;
H is the elastic modulus with respect to a change in matric suction ($u_a - u_w$);
ΔV_w is the change in the volume of water in the soil element;
m_1^w is the water volume change modulus with respect to a change in the net normal stress; and
m_2^w is the water volume change modulus with respect to a change in matric suction.

Fig. 4. Three-dimensional constitutive surface for the soil structure of an unsaturated soil (from Fredlund 1981).

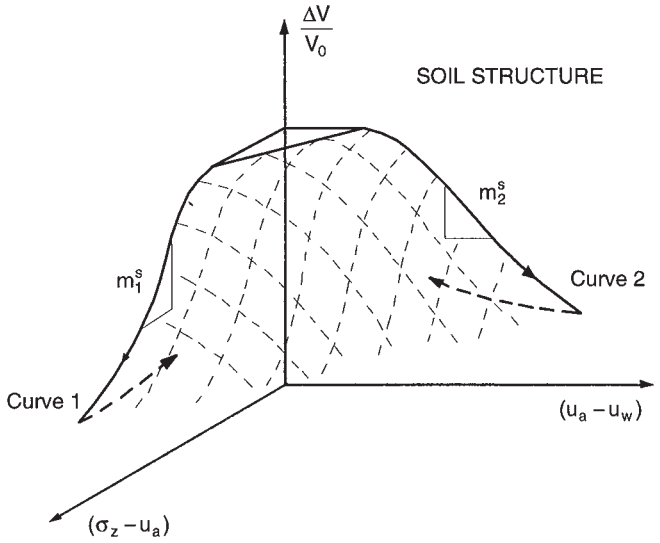

Fig. 5. Three-dimensional constitutive surface for the water phase of an unsaturated soil (from Fredlund 1981).

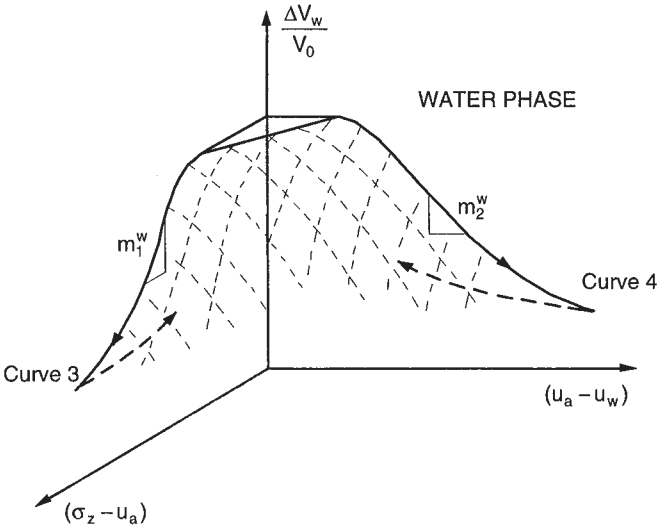

The relationships between the variables in [2] and [3] are shown in Figs. 4 and 5, respectively.

Continuity requirement for water phase

The equation of continuity for the water phase in a soil takes the following form (Freeze and Cherry 1979):

$$[4] \qquad \frac{\partial}{\partial t}\left(\frac{V_w}{V_0}\right) = -\frac{\partial q_w}{\partial z}$$

where

V_w is the water volume in the soil element;
V_w/V_0 is the net water volume change per unit volume of the soil element; and
q_w is the water flow rate across a unit area of the soil element in the z direction.

Darcy's law can be applied to the flow of water through an

unsaturated soil (Buckingham 1907; Richards 1931; Childs and Collis-George 1950).

$$[5] \quad q_w = -k_w(u_w)\frac{\partial h_w}{\partial z}$$

where

$k_w(u_w)$ is the coefficient of permeability with respect to the water phase in the z direction (which is a function of the negative pore-water pressure);
h_w is the hydraulic head (i.e., gravitational, pore-water pressure, and velocity heads or $z + (v_w^2/2g) + (u_w/\rho_w g)$);
z is the elevation;
v_w is the velocity;
u_w is the pore-water pressure;
ρ_w is the density of water;
g is the gravitational acceleration; and
$\partial h_w/\partial z$ is the hydraulic head gradient in the z direction.

Substituting Darcy's law for the flow rate of water, q_w, into [4] gives

$$[6] \quad \frac{\partial}{\partial t}\left(\frac{V_w}{V_0}\right) = \frac{\partial}{\partial z}\left(k_w\frac{\partial h_w}{\partial z}\right)$$

Assuming the thickness of the sample is small and the water velocity head in the sample is negligible, the continuity equation for the water phase can be written as

$$[7] \quad \frac{\partial}{\partial t}\left(\frac{V_w}{V_0}\right) = \frac{1}{\rho_w g}\frac{\partial}{\partial z}\left(k_w\frac{\partial u_w}{\partial z}\right)$$

Derivation of the governing equations for swelling tests

The following assumptions are made to simplify the derivation of the governing equation for a swell test: (*i*) isotropic soil; (*ii*) infinitesimal strain; (*iii*) linear constitutive relations for a small change in net normal stress or matric suction; (*iv*) the coefficient of permeability of water is constant for a small change in matric suction; and (*v*) the permeability with respect to the air phase, k_a, is significantly greater than the permeability with respect to the water phase, k_w, which means that the pore-air pressure is always equal to the surrounding air pressure (i.e., $u_a = 0$). According to assumption *v* the net normal stress ($\sigma_z - u_a$) becomes equal to the total vertical stress σ_z, and matric suction ($u_a - u_w$) becomes equal to the negative pore-water pressure u_w. As a result of the above assumptions, the constitutive equations for an unsaturated soil become

$$[8] \quad \varepsilon_z = \frac{\Delta V_v}{V_0} = m_1^s\Delta\sigma_z - m_2^s\Delta u_w$$

$$[9] \quad \frac{\Delta V_w}{V_0} = m_1^w\Delta\sigma_z - m_2^w\Delta u_w$$

Governing differential equation for constant load oedometer test

The total vertical stress σ_z is maintained constant during the constant-load test (i.e., $\Delta\sigma_z = 0$). As a result, the constitutive equations for an unsaturated soil (i.e., eqs. [8] and [9]) can be simplified as

$$[10] \quad \varepsilon_z = \frac{\Delta V_v}{V_0} = -m_2^s\Delta u_w$$

$$[11] \quad \frac{\Delta V_w}{V_0} = -m_2^w\Delta u_w$$

The continuity requirement for the water phase during the constant-load test is given by [7]. Substituting [11] into [7] and noting that the incremental change in pore-water pressure with time is equal to the actual pore-water pressure change (i.e., $(\partial\,\Delta u_w)/(\partial t) = (\partial\, u_w)/(\partial t)$) gives

$$[12] \quad \frac{\partial u_w}{\partial t} = -\frac{1}{\rho_w g m_2^w}\frac{\partial}{\partial z}\left(k_w\frac{\partial u_w}{\partial z}\right)$$

Equation [12] is a transient water flow equation for the constant-load test. It can be used to compute the negative pore-water pressure at different depths and times during the constant-load swelling process. The negative pore-water pressure change, Δu_w, computed from [12] can be substituted into the soil volume change equation (eq. [10]) to calculate the strain, ε_z, during the constant-load test.

The transient water flow (eq. [12]) reverts to Terzaghi's consolidation equation for saturated soils if the coefficient of water volume change, m_2^w, in [12] is replaced by the coefficient of volume change, m_v.

$$[13] \quad \frac{\partial u_w}{\partial t} = \frac{k_w}{\rho_w g m_v}\frac{\partial^2 u_w}{\partial z^2}$$

where m_v is the coefficient of volume change for a saturated soil. However, it should be noted that the coefficient of permeability, k_w, in [12] is not a constant but varies significantly with the degree of saturation (or the water content) in the soils. The change in void ratio may have a secondary affect on the coefficient of permeability (Fredlund 1982).

Governing differential equation for constant-volume oedometer test

The swelling tests primarily involve two processes, namely the transient water flow process and the soil volume change process. Two equations are required to describe the two processes.

During the constant-load oedometer test, the total stress is maintained constant and only a change in water content due to transient water flow can cause a change in negative pore-water pressure and consequently a change in soil volume. Therefore, the change in pore-water pressure can be calculated using only the transient water flow equation (i.e., eq. [12]). Then, the change in pore-water pressure computed using [12] is substituted into the soil volume change equation (i.e., eq. [10]) to obtain the volume change. In other words, the transient water flow equation and the soil volume change equation can be solved separately to simulate the constant-load test.

During the constant-volume test, the total stress increases with respect to time. The increase in the total stress results in a tendency for the soil to decrease its volume and hence results in a decrease in the negative pore-water pressure. Alternatively, the water content increase due to transient water flow causes the negative pore-water pressure to decrease. The decrease in the negative pore-water pressure results in a tendency

for the soil to increase in volume and consequently results in a further increase in the total stress because of the requirement to maintain a constant volume. Therefore, it is difficult to separate the two processes (i.e., the transient water flow process and the soil volume change process) during the constant volume test. To simulate the constant-volume test, the simultaneous equations coupling the transient water flow process with the soil volume change process must be formulated.

Differential equation for water flow

The continuity requirement for the water phase is given by [7], and the constitutive relation for the water phase of an unsaturated soil is given by [9].

Substituting [9] into [7] gives

$$[14] \quad m_1^{w}\frac{\partial \sigma_z}{\partial t} - m_2^{w}\frac{\partial u_w}{\partial t} = \frac{1}{\rho_w g}\frac{\partial}{\partial z}\left(k_w\frac{\partial u_w}{\partial z}\right)$$

Differentiating [8] with respect to time yields

$$[15] \quad \frac{\partial \varepsilon_z}{\partial t} = m_1^{s}\frac{\partial \sigma_z}{\partial t} - m_2^{s}\frac{\partial u_w}{\partial t}$$

Equation [15] can be rewritten as

$$[16] \quad \frac{\partial \sigma_z}{\partial t} = \frac{1}{m_1^{s}}\left(\frac{\partial \varepsilon_z}{\partial t} + m_2^{s}\frac{\partial u_w}{\partial t}\right)$$

Substituting [16] into [14] gives

$$[17] \quad \frac{m_1^{w}}{m_1^{s}}\frac{\partial \varepsilon_z}{\partial t} - \left(m_2^{w} - \frac{m_2^{s}m_1^{w}}{m_1^{s}}\right)\frac{\partial u_w}{\partial t} = \frac{1}{\rho_w g}\frac{\partial}{\partial z}\left(k_w\frac{\partial u_w}{\partial z}\right)$$

Written in terms of displacement, the strain in the z direction can be expressed as

$$[18] \quad \varepsilon_z = \frac{\partial \delta_z}{\partial z}$$

where δ_z is the displacement in the z direction.

Substituting the strain in [18] into [17] gives

$$[19] \quad \frac{m_1^{w}}{m_1^{s}}\frac{\partial}{\partial t}\left(\frac{\partial \delta_z}{\partial z}\right) - \left(m_2^{w} - \frac{m_2^{s}m_1^{w}}{m_1^{s}}\right)\frac{\partial u_w}{\partial t} = \frac{1}{\rho_w g}\frac{\partial}{\partial z}\left(k_w\frac{\partial u_w}{\partial z}\right)$$

Equation [19] can be rewritten as

$$[20] \quad \alpha\frac{\partial}{\partial t}\left(\frac{\partial \delta_z}{\partial z}\right) - \beta\frac{\partial u_w}{\partial t} = \frac{1}{\rho_w g}\frac{\partial}{\partial z}\left(k_w\frac{\partial u_w}{\partial z}\right)$$

where

$$\alpha = \frac{m_1^{w}}{m_1^{s}}$$

$$\beta = m_2^{w} - \frac{m_2^{s}m_1^{w}}{m_1^{s}}$$

Equation [20] is the transient flow equation for the water phase in terms of displacement and negative pore-water pressure.

Differential equation for soil volume change

The constitutive relation for the volumetric strain of an unsaturated soil for the one-dimensional case is given by [8], and the deformation equation for the one-dimensional case by [18]. Substituting the strain in [18] into [8] allows the displacement to be written as

$$[21] \quad \frac{\partial \delta_z}{\partial z} = m_1^{s}\Delta\sigma_z - m_2^{s}\Delta u_w$$

Rearranging [21] results in

$$[22] \quad \Delta\sigma_z = \frac{1}{m_1^{s}}\frac{\partial \delta_z}{\partial z} + \frac{m_2^{s}}{m_1^{s}}\Delta u_w$$

Substituting [22] into the force equilibrium equation (i.e., eq. [1]) and differentiating it with respect to z gives

$$[23] \quad \frac{\partial^2 \delta_z}{\partial z^2} = -m_2^{s}\frac{\partial u_w}{\partial z}$$

Equation [23] is a soil volume change equation for the constant-volume oedometer test.

Simultaneous equations for the constant-volume oedometer test

The soil volume change equation and the transient water flow equation for the constant-volume test are given by [23] and [20], respectively. Equation [20] is used to define the negative pore-water pressure, u_w, when solving for soil volume change in [23]. The displacement δ_z required in [20] depends on the soil volume change given by [23]. Equations [23] and [20] must be solved simultaneously.

The governing equations for the constant-volume test, [23] and [20], can be written in the form of simultaneous equations as follows:

$$[24] \quad \left\{\begin{array}{l} \dfrac{\partial^2 \delta_z}{\partial z^2} = -m_2^{s}\dfrac{\partial u_w}{\partial z} \\ \alpha\dfrac{\partial}{\partial t}\left(\dfrac{\partial \delta_z}{\partial z}\right) = \dfrac{1}{\rho_w g}\dfrac{\partial}{\partial z}\left(k_w\dfrac{\partial u_w}{\partial z}\right) + \beta\dfrac{\partial u_w}{\partial t} \end{array}\right\}$$

There are two unknowns (i.e., δ_z and u_w) in [24] and two equations. Therefore, these equations can be used to compute the negative pore-water pressure and displacement at various depths and times during the constant-volume swelling process. The negative pore-water pressure change, Δu_w, and the displacement, δ_z, computed from [24] can be substituted into [22] to calculate the change in vertical stress, $\Delta\sigma_z$, applied to the soil surface during the constant-volume test. The relationships required to solve [24] are the compression or rebound curve (i.e., V_w/V_0 versus $(\sigma_z - u_a)$), the soil-water characteristic curve, the shrinkage or swelling curve, and the permeability function (i.e., $k_w(u_w)$).

Since the constant-load swelling process can be seen as a particular case of the constant-volume swelling process, in which the total stress is maintained constant, the simultaneous equations (eq. [24]) can also be used to simulate the constant-load swelling process.

In summary, to simulate various swelling testing procedures, the coupled soil volume change and transient water flow equations (i.e., eqs. [23] and [20]) should be solved simultaneously in the domain of the soil profile with respect to space and time under different boundary conditions.

Numerical solution

The governing differential equation describing the pore-pressure and volume-change behaviour during various swelling tests (i.e., eqs. [23] and [20]) is nonlinear. The coefficients of permeability, k_w, the coefficients of soil volume change, m_1^s and m_2^s, and the coefficients of water volume change, m_1^w and m_2^w, vary with vertical position and time due to changes in total stress, and negative pore-water pressure. A closed-form solution is not available, therefore a numerical solution is presented.

To obtain a numerical solution, [23] and [20] must be discretized in terms of both time and space. The spatial discretization is performed using Galerkin's weighted residual method. The Euler (i.e., Back-difference) approximation is utilized to perform the time discretization.

The finite element formulation for [23] and [20] is given in matrix form as follows (Shuai 1996):

$$[25]\quad \begin{bmatrix} \bar{\boldsymbol{K}} & \boldsymbol{K}' \\ \boldsymbol{K} & \tilde{\boldsymbol{K}} \end{bmatrix} \begin{Bmatrix} \delta \\ \Delta\eta \end{Bmatrix} = \begin{Bmatrix} \boldsymbol{R} \\ \boldsymbol{S} \end{Bmatrix}$$

where for each element

$$[\bar{\boldsymbol{K}}] = \frac{1}{l m_1^s} \begin{bmatrix} 1 & -1 \\ -1 & 1 \end{bmatrix}$$

$$[\boldsymbol{K}'] = \frac{m_2^s}{2 m_1^s} \begin{bmatrix} -1 & -1 \\ 1 & 1 \end{bmatrix}$$

$$[\boldsymbol{K}] = \frac{\alpha}{2} \begin{bmatrix} -1 & 1 \\ -1 & 1 \end{bmatrix} = \frac{m_1^w}{2 m_1^s} \begin{bmatrix} -1 & 1 \\ -1 & 1 \end{bmatrix}$$

$$[\tilde{\boldsymbol{K}}] = -([\boldsymbol{G}] - \Delta t[\boldsymbol{C}]) = -\frac{\beta l}{2} \begin{bmatrix} 1 & 0 \\ 0 & 1 \end{bmatrix} + \frac{k_w \Delta t}{\rho_w g l} \begin{bmatrix} 1 & -1 \\ -1 & 1 \end{bmatrix}$$

$$= -\frac{1}{2} \begin{bmatrix} \beta l - \dfrac{2k_w \Delta t}{\rho_w g l} & \dfrac{2k_w \Delta t}{\rho_w g l} \\ \dfrac{2k_w \Delta t}{\rho_w g l} & \beta l - \dfrac{2k_w \Delta t}{\rho_w g l} \end{bmatrix}$$

$$[\boldsymbol{R}] = \begin{bmatrix} R_1 \\ R_2 \end{bmatrix}$$

$$[\boldsymbol{S}] = [\boldsymbol{K}]\{\delta\}_1 - [\boldsymbol{G}]\{\Delta\eta\}_t - \Delta t[\boldsymbol{C}]\{\eta\}_0 + \Delta t\{\boldsymbol{Q}\}_{t+\Delta t}$$

$$= \frac{m_1^w}{2 m_1^s} \begin{bmatrix} -1 & 1 \\ -1 & 1 \end{bmatrix} \begin{Bmatrix} \delta_1^t \\ \delta_2^t \end{Bmatrix} - \frac{\beta l}{2} \begin{bmatrix} 1 & 0 \\ 0 & 1 \end{bmatrix} \begin{Bmatrix} \Delta\eta_1^t \\ \Delta\eta_2^t \end{Bmatrix} - \frac{k_w \Delta t}{\rho_w g l} \begin{bmatrix} 1 & -1 \\ -1 & 1 \end{bmatrix} \begin{Bmatrix} \eta_1^0 \\ \eta_2^0 \end{Bmatrix} + \Delta t\{\boldsymbol{Q}\}_{t+\Delta t}$$

$$= \begin{cases} \dfrac{m_1^w}{2 m_1^s}\left(\delta_2^t - \delta_1^t\right) - \dfrac{\beta l}{2}\Delta\eta_1^t + \dfrac{k_w \Delta t}{\rho_w g l}\left(\eta_2^1 - \eta_1^0\right) + Q_1^{t+\Delta t}\Delta t \\ \dfrac{m_1^w}{2 m_1^s}\left(\delta_2^t - \delta_1^t\right) - \dfrac{\beta l}{2}\Delta\eta_2^t + \dfrac{k_w \Delta t}{\rho_w g l}\left(\eta_1^0 - \eta_2^0\right) + Q_2^{t+\Delta t}\Delta t \end{cases}$$

where

l is the length of the element;
δ is the value of the displacement at the node;
η is the value of the negative pore-water pressure at the node;
R is the external forces applied on the node;
Q is the net flux of water entering the system at the node;
ρ_w is water density (kg/m^3); and
g is gravitational acceleration (m/s^2).

A computer program SWELL was developed based on [25] for predicting the pore-water pressure and volume-change behaviour during a swell test.

Theoretical simulation of oedometer swelling test

The proposed theoretical model was used to simulate the results from several oedometer swelling tests (i.e., free-swell, constant-volume, constant water content or undrained-loading, and loaded-swell oedometer tests) on the compacted Regina Clay.

Regina Clay is a highly swelling, postglacial lake deposit found in the city of Regina, Saskatchewan. Regina Clay was statically compacted to produce a specimen with a initial void ratio of 0.96 and a molding water content of 26%, slightly less than the optimum water content of 28.5%. The initial matric suction at a water content of 26% was 575 kPa, which was measured using a null-type pressure plate test (Fredlund and Rahardjo 1993).

Calculation parameters

The solution to the governing equation (eq. [24]) requires the following soil properties: coefficient of permeability function, k_w; coefficients of soil structure volume change, m_1^s and m_2^s; and coefficients of water volume change, m_1^w and m_2^w.

Several types of laboratory tests were performed to independently measure the above soil properties. These tests are the falling-head permeability test, the free-swell oedometer test, the pressure-plate test, the shrinkage test, and the constant-suction consolidation test. The measured saturated coefficients of permeability versus void ratio relationship from two saturated, falling-head permeability tests are presented in Fig. 6. The coefficient of permeability function is shown in Fig. 7. This function was computed indirectly from the measured soil-water characteristic curve and the measured saturated coefficient of permeability of the soil (Fredlund and Rahardjo 1993). The measured three-dimensional constitutive surfaces for the soil structure and the water phase are presented in Figs. 8 and 9, respectively.

According to the test results, several equations were proposed to describe the soil coefficients required to solve [24] (Shuai 1996). A summary of the soil coefficients and the magnitudes used in the theoretical simulation is given in Table 1. All of the coefficients were obtained from independent laboratory test results. Detailed information regarding the independent measurement of the coefficients is available in Shuai (1996).

Comparison between theoretical simulation and laboratory test results

The values of the coefficients listed in Table 1 were used in the computer program SWELL to simulate the various oedometer

Table 1. A summary of the coefficients to be used in theoretical simulations.

Coefficient	Functions	Values of parameters
k_w	$k_w = \frac{k_o\, e^b}{1 + a\left(\frac{u_a - u_w}{\rho_w g}\right)^n}$	$k_o = 0.4 \times 10^{-10}$ m/s $b = 18.5$ $a = 0.01$ $n = 1.1$
m_1^s (C_t)	$m_1^s = m_{10}^s (u_a - u_w)^{-c_a}$	$m_{10}^s = 4.06 \times 10^{-4}$ $(\sigma - u_a \le 100$ kPa) $C_{t0} = 0.276$ $(\sigma - u_a > 100$ kPa) $c_a = \frac{(u_a - u_w)}{c_{a1} + c_{a2}(u_a - u_w)}$ $c_{a1} = 86.9$ $c_{a2} = 3.45$
m_{ls}^s (C_{ts})	$C_{ts} = 0.0645$	
m_2^s (C_m)	$m_2^s = m_{21}^s + m_{22}^s$ $m_{22}^s = \frac{c_b}{(u_a - u_w)}$	$C_{m1} = 0.0676$ $(u_a - u_w \le 12$ kPa) $C_{m1} = 0.0803$ $(u_a - u_w > 12$ kPa) $c_b = \frac{(\sigma - u_a)}{c_{b1} + c_{b2}(\sigma - u_a)}$ $c_{b1} = 14\,027$ $c_{b2} = 28.18$
$m_1^w(D_t)$	$m_1^w = m_1^s$ $(u_a - u_w \le 1$kPa) $m_1^w = m_1^s (u_a - u_w)^{c_e}$ $(u_a - u_w \ge 1$kPa)	$c_e = -0.28$
$m_2^w(D_m)$	$D_m = D_{mo} \exp[c_d(\sigma - u_a)]$	$D_{m0} = 0.0410$ $c_d = -0.0027$

Note: Parameters are defined as follows: a, c_{a1}, c_{a2}, c_{b1}, c_{b2}, and c_d are empirical constants; n, b, c_a, and c_e are empirical indices; e is the void ratio; $m_1^s$is the soil structure volume change modulus with respect to a change in net normal stress; $m_{10}^s$is the soil structure volume change modulus with respect to a change in net normal stress at zero matric suction; C_t is the compressive index with respect to net normal stress; C_{ts} is the swell index with respect to net normal stress; m_2^s is the soil structure volume change modulus with respect to a change in matric suction; m_{22}^s is a pseudo-coefficient of volume change with respect to matric suction which is used to take into account the increase in compressibility caused by decreasing the matric suction; $m_{21}^s$is the coefficient of volume change with respect to matric suction (i.e., $(1 + \mu)/H(1 - \mu)$; eq. [2]); C_m is the compressive index with respect to matric suction; c_b is the slope of the volumetric strain due to an increase in compressibility versus matric suction curve on a semi-natural-logarithm scale; D_t is the water content index with respect to net normal stress; D_m is the water content index with respect to matric suction; and D_{m0} is the water content index with respect to matric suction at zero net normal stress.

swelling tests (i.e., constant water content or undrained loading, free-swell, constant-volume, and loaded- swell tests). The comparisons between theoretical simulation and laboratory test results for those tests are presented in the following sections.

Constant water content or undrained loading test

Estimating the initial condition leading to a swelling test after the application of an external load requires an examination of undrained loading. The simulation of undrained loading was started by specifying a zero flux boundary for the top of the specimen and a zero flux and zero displacement boundary for the bottom. A uniform initial matric suction of 575 kPa was specified for all nodes. This initial suction was set equal to the measured suction in the specimen. The initial stress for all elements was equal to the applied token load (i.e., 1 kPa). During the simulation, external load acting on the top of the specimen was increased step by step until a predetermined maximum load was reached.

The computed matric suction versus applied load relationship is shown in Fig. 10 and exhibits a nonlinear relationship at degrees of saturation less than 100% (i.e., $(u_a - u_w) > 0$ kPa). The pore-water response is low at the beginning of the test due to the low degree of saturation. The pore-water pressure response becomes more significant when the pore-water pressures approach zero (i.e., at higher degrees of saturation). When the specimen becomes saturated, the relationship between pore-water pressure and the total vertical stress becomes linear and parallel to a pore-pressure parameter of 1 (i.e., $\Delta u_w/\Delta\sigma = 1$). In other words, at saturation a change in total vertical stress under undrained conditions produces an equal change in pore-water pressure.

Comparing with the measured values (Fig. 11) published by Bishop (1954), the calculation results appear reasonable. The calculated pore-water pressure parameters for K_o-loading conditions, B_w, range from 0.2 to 0.6, which agrees closely with typical values suggested by Skempton (1954).

The computed and measured void ratio versus applied load relationships are shown in Fig. 12. A comparison between the computed and measured curves shows reasonably good agreement for the greater part of the test (i.e., $(\sigma - u_a) \le 400$ kPa). Discrepancies were noted between the computed and measured curves when the net normal stress was greater than 400 kPa. The poorer agreement can be attributed to the fact that some coefficients (e.g., c_a and c_b) used in modelling were obtained from laboratory tests with a maximum net normal stress of 400 kPa due to a limitation in the test equipment.

Free-swell oedometer test

Computer simulations of the free-swell oedometer testing process were carried out by specifying a zero flux boundary for the top of the specimen and a zero pore-water pressure and zero displacement for the bottom. A uniform initial matric suction of 575 kPa was specified for all nodes. The initial stress for all elements was equal to the applied token load. Since the surcharge load was kept constant (i.e., token load) during the test, only some of the parameters (i.e., k_w, C_m or m_2^s, and D_m or m_2^w) are required in the analysis. The remaining parameters do not have any effect on the calculations.

Figure 13 shows the measured and computed deflection versus time curves for two 100 mm high specimens and two 20 mm high specimens. A comparison between the computed and measured curves shows reasonably good agreement for the full length of the test for these specimens. The predicted and measured total heaves are almost the same.

After a period of time from the start of the test (i.e., 1000 min for a 100 mm high specimen), the slope of the deflection versus time curves increases significantly. This increase is mainly due to an increase of the coefficient of permeability of the specimen as a result of a decrease in matric suction.

Fig. 6. Saturated coefficient of permeability versus void ratio for the falling-head permeability tests FHPT1 and FHPT2.

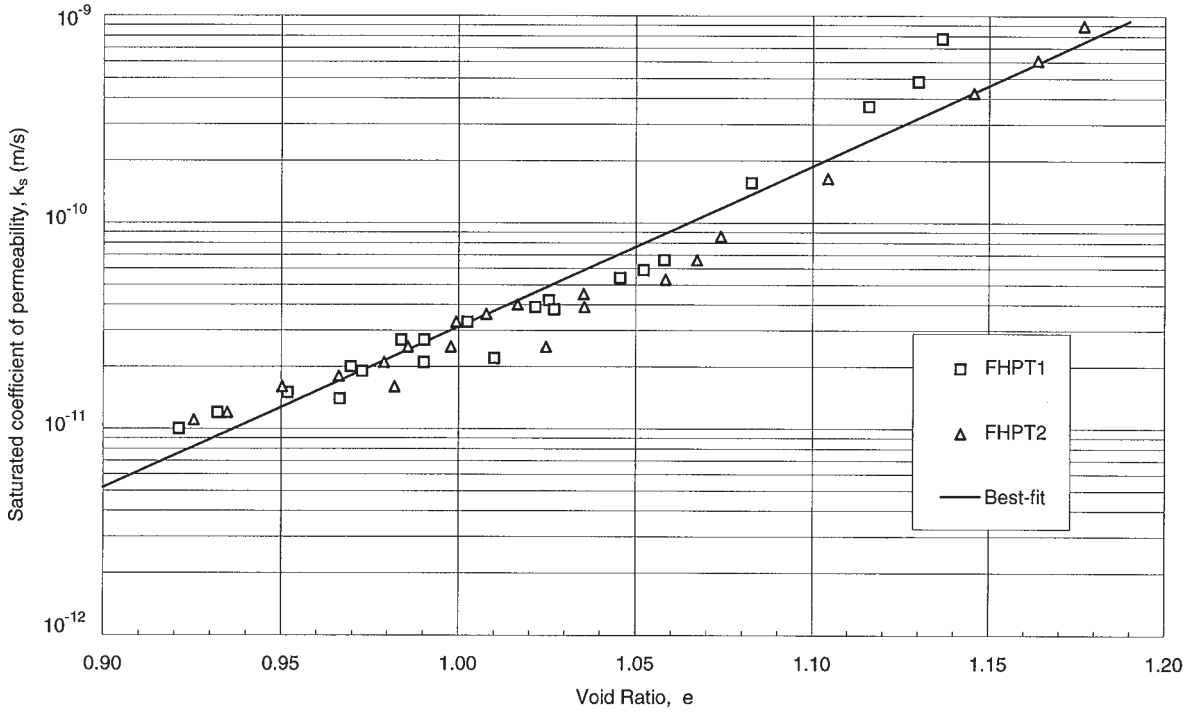

Fig. 7. Unsaturated coefficient of permeability function for compacted Regina Clay.

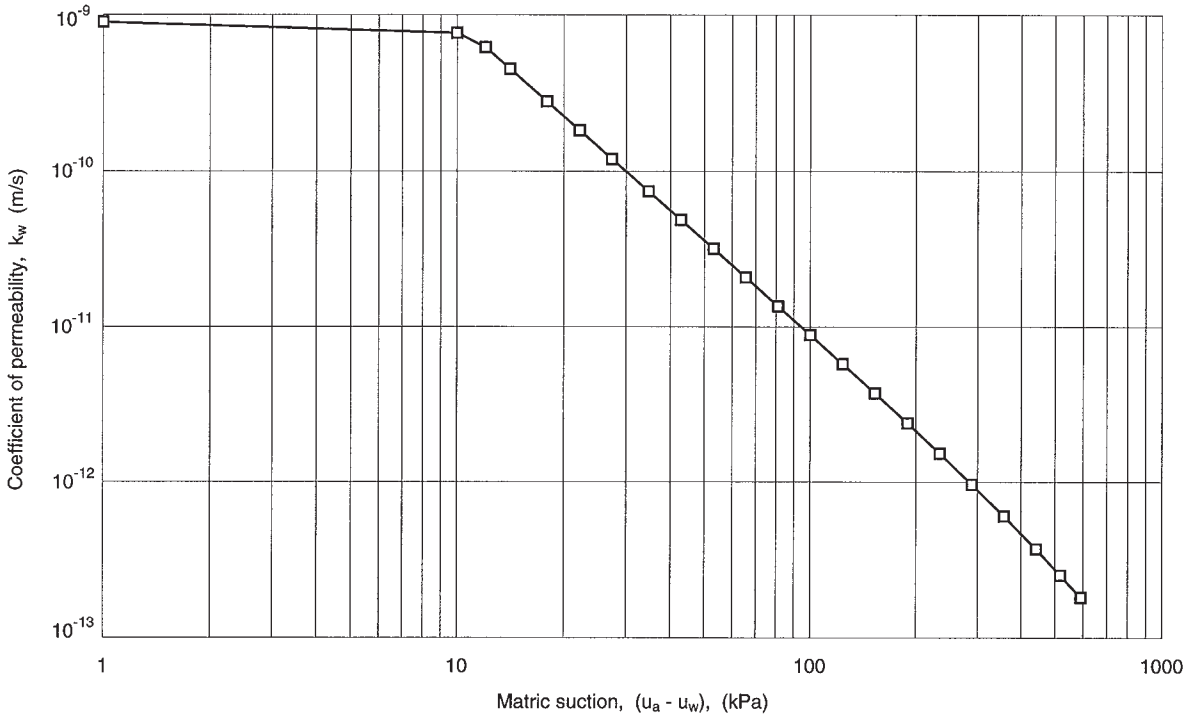

All curves show that the total heave is proportional to the height of the specimen. The rate of swell is independent of the height. The duration of swelling for the specimens with a height of 100 mm is about 25 times longer than that required for the specimen with a height of 20 mm. In other words, the duration for swelling is proportional to the square of the overall height. The longer duration of swelling for a thicker specimen is a result of the longer drainage path for the dissipation of pore-water pressure.

The measured and computed void ratio versus applied load

Fig. 8. Measured soil structure constitutive surface for compacted Regina Clay.

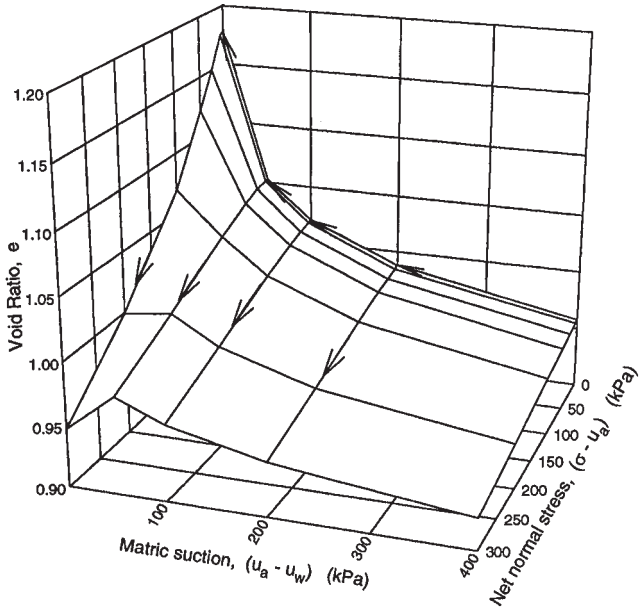

Fig. 9. Measured water phase constitutive surface for compacted Regina Clay.

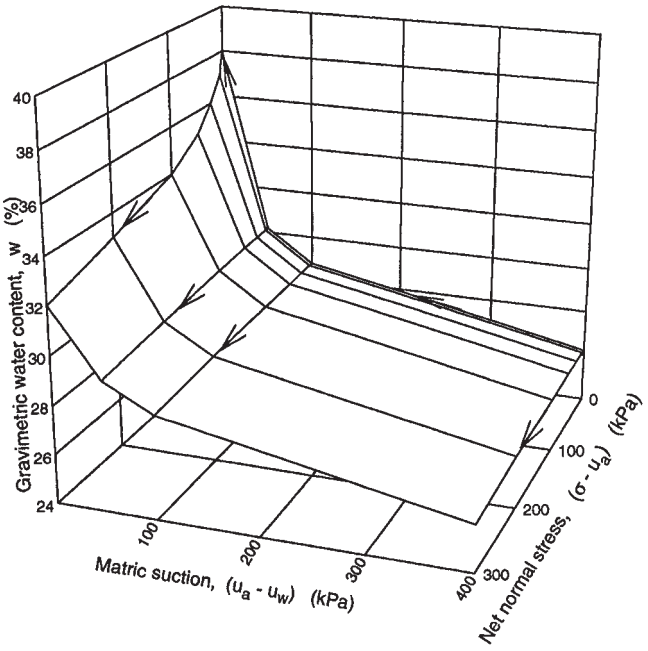

Fig. 10. Computed pore-water pressure versus total vertical pressure curves for constant water content (undrained loading) test.

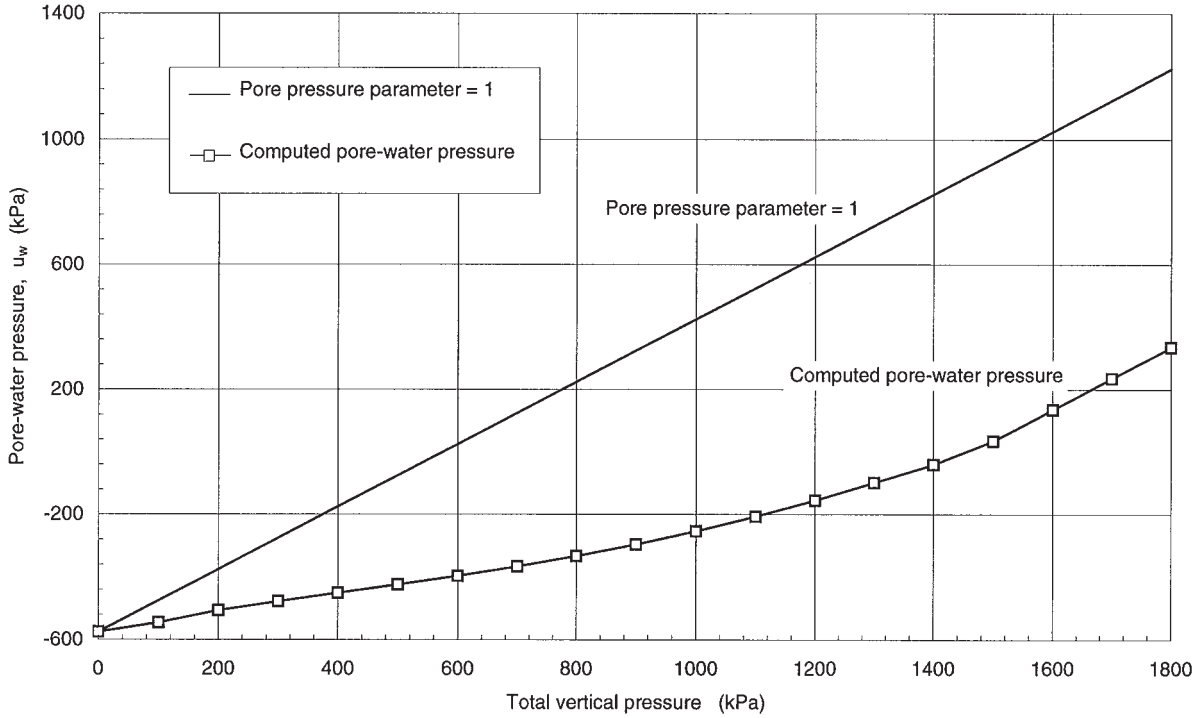

relationships are shown in Fig. 14. The intersection of the computed void ratio versus applied load curve with the initial void ratio line (i.e., e of 0.960) gives a swelling pressure of 300 kPa. This value for swelling pressure is close to the measured swelling pressure from the free swell test (i.e., 320 kPa).

A comparison between the computed and measured matric suction profiles for the 100 mm high specimen is presented in Fig. 15. The matric suction was measured by placing Whatman No. 42 filter papers between each layer of specimen and measuring the water content of the filter papers after the test. Good agreement was found between the measured and computed matric suctions for the early (i.e., t = 1500 min) and later stages (i.e., t = 54 700 min) of the test. Some differences were noted during the middle stage (i.e., t = 5300 min) of the test. The matric suctions predicted at the upper part of the specimen are somewhat lower than the measured suctions. The poor

Fig. 11. Pore pressure versus total major principal stress (from Bishop 1954).

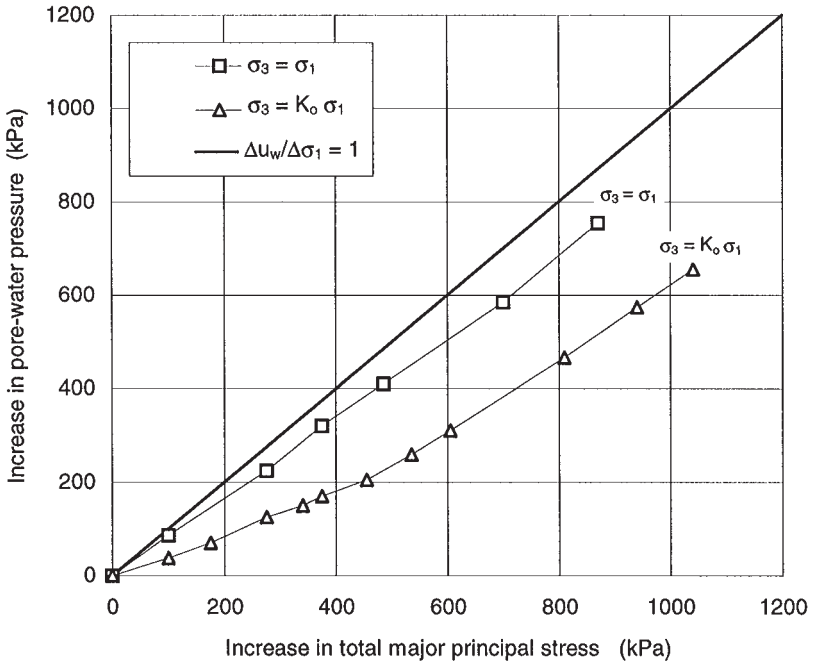

Fig. 12. Computed and measured void ratio versus net normal stress curves for constant water content tests.

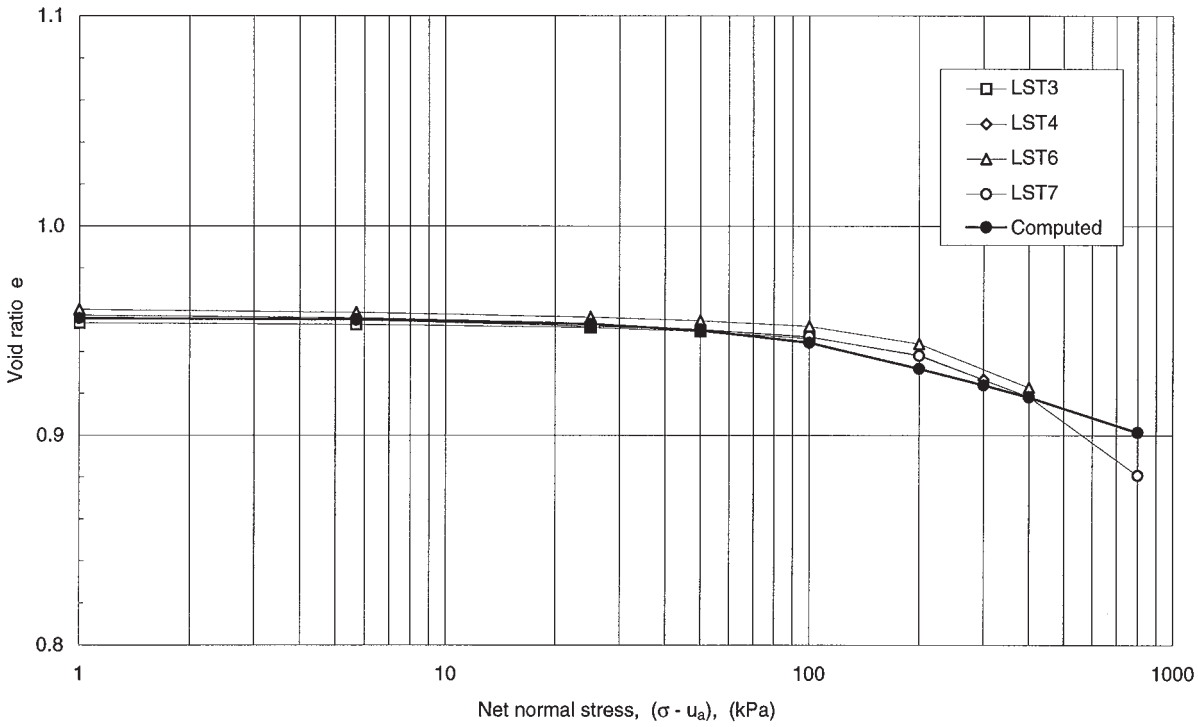

prediction could be attributed to the filter paper placed in the specimen. Since the water retentivity of the filter paper is much higher than that of the soil, the filter paper may absorb more water than the soil for a given decrease in matric suction. As a result, the filter papers in the soil slow the advance of the saturated zone resulting in a slower decrease of matric suction.

Good agreement was observed between the measured and computed profiles of deformation (Fig. 16).

Constant-volume oedometer test

To simulate the constant-volume oedometer test, a zero flux and zero displacement boundary were specified for the top of the specimen and a zero pore-water pressure and zero displacement were specified for the bottom of the specimen. A uniform initial matric suction of 575 kPa was specified for all nodes. The initial stress for all elements was equal to a token load (i.e., 1 kPa).

Fig. 13. Computed and measured deflection versus time curves for free-swell oedometer tests.

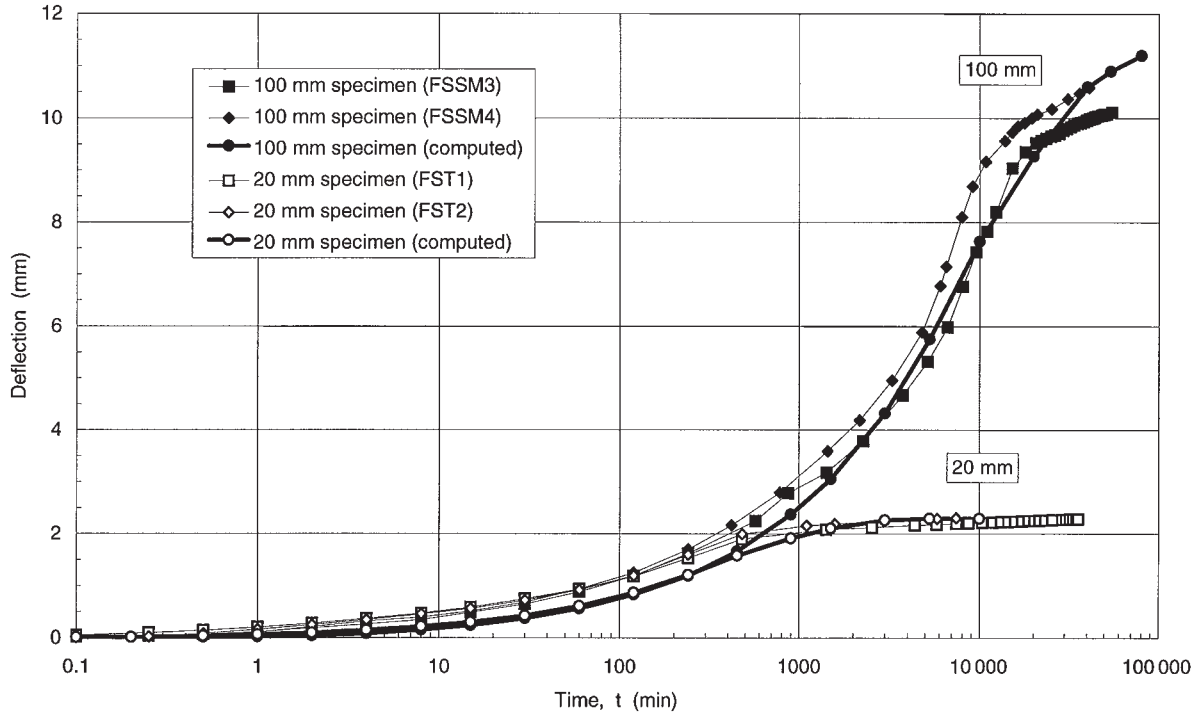

Fig. 14. Computed and measured void ratio versus net normal stress curves for free-swell oedometer tests.

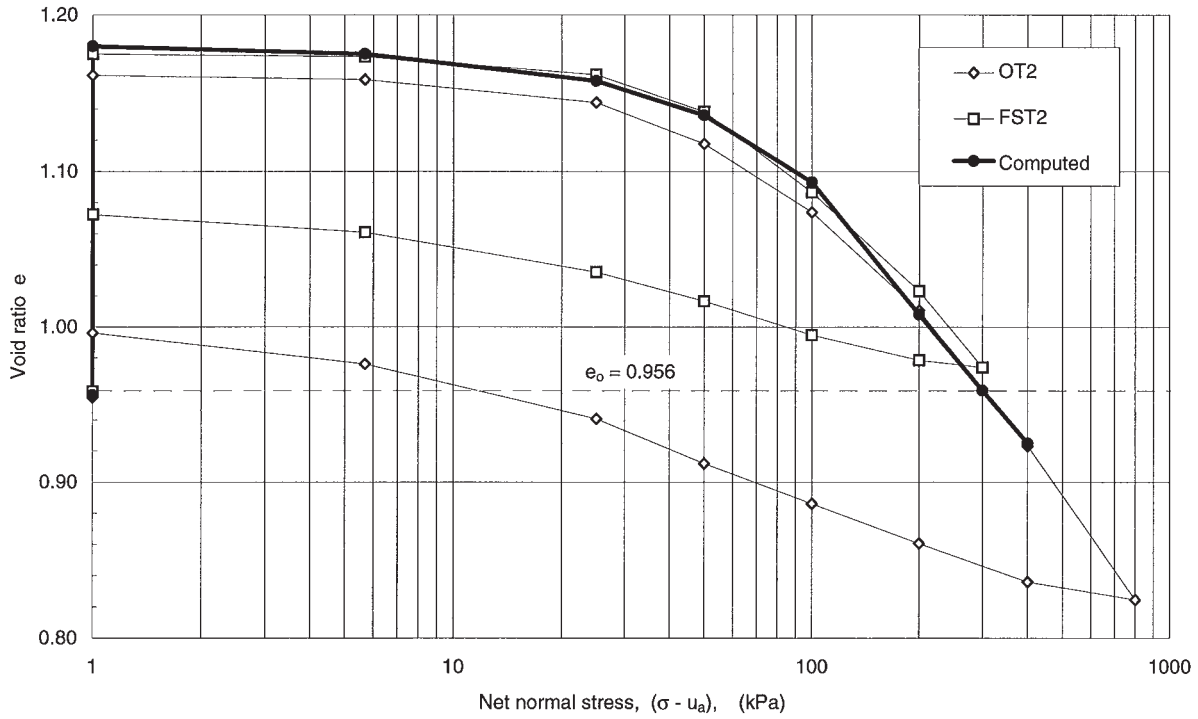

The measured and computed vertical total stress versus time curves for two 100 mm high specimens and two 20 mm high specimens are shown in Fig. 17. A comparison of the computed and measured curves shows reasonably good agreement for the full duration of the test for all specimens.

All curves show that with an increase in the height of the specimen, the rate of swelling pressure development decreases while the duration of swelling increases. Both the computed and measured curves show that the swelling pressures for both specimens are essentially the same.

Fig. 15. Computed and measured matric suction profiles for free-swell oedometer test.

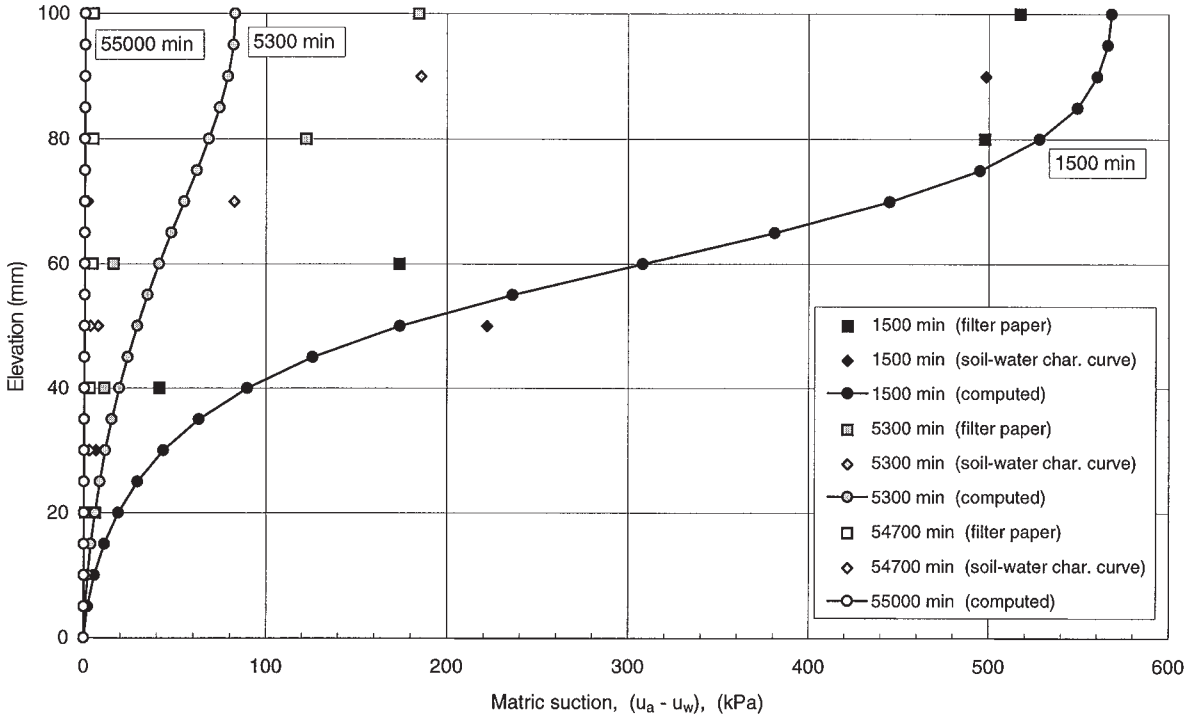

Fig. 16. Computed and measured deformation profiles for free-swell oedometer test.

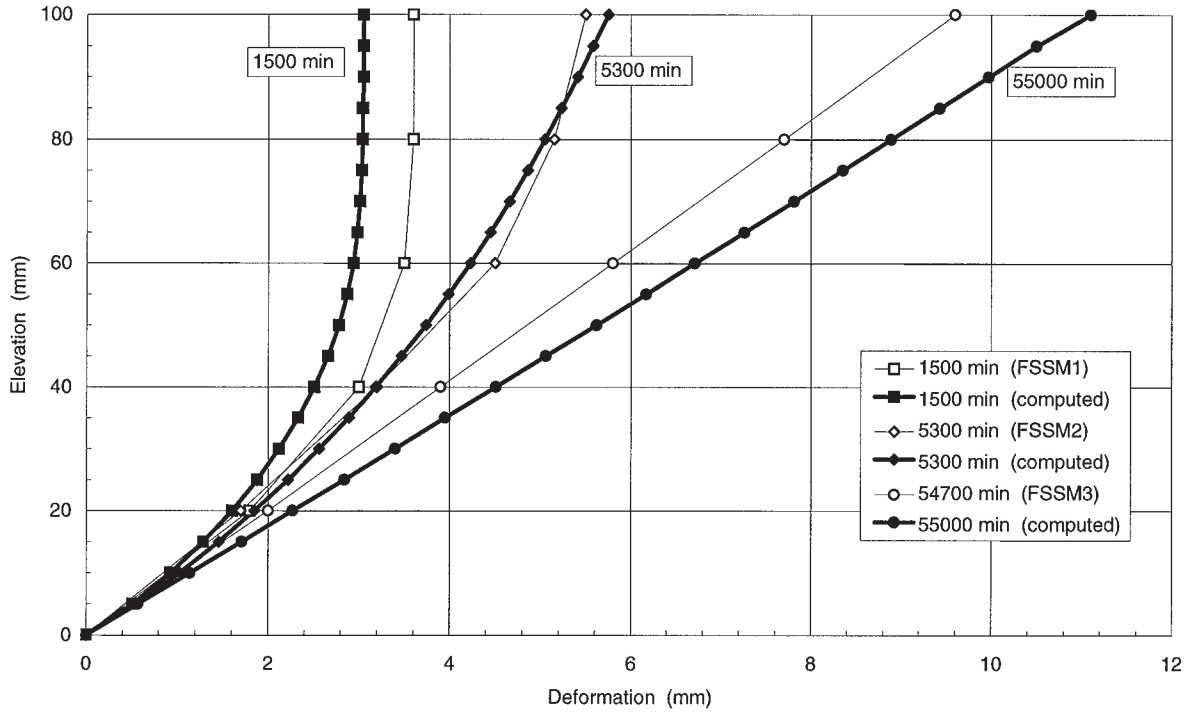

The predicted swelling pressure (i.e., 293 kPa) is somewhat higher than the measured "uncorrected" swelling pressure (i.e., 265 kPa for the 20 mm high specimen and 237 kPa for the 100 mm high specimen). However, the predicted value is close to the "corrected" swelling pressure (i.e., 300 kPa). This difference may be attributed to the influence of sampling disturbance during sample preparation. In addition, the predicted vertical stress during the early stages of the test is somewhat higher than the measured vertical stress for the 20 mm high specimen. This may be attributed to the fact that, during the test, the null-type measuring system used in this test is sensitive to small amounts of swelling (i.e., 0.005 mm) which may

Fig. 17. Computed and measured vertical net normal stress versus time curves for constant-volume oedometer test.

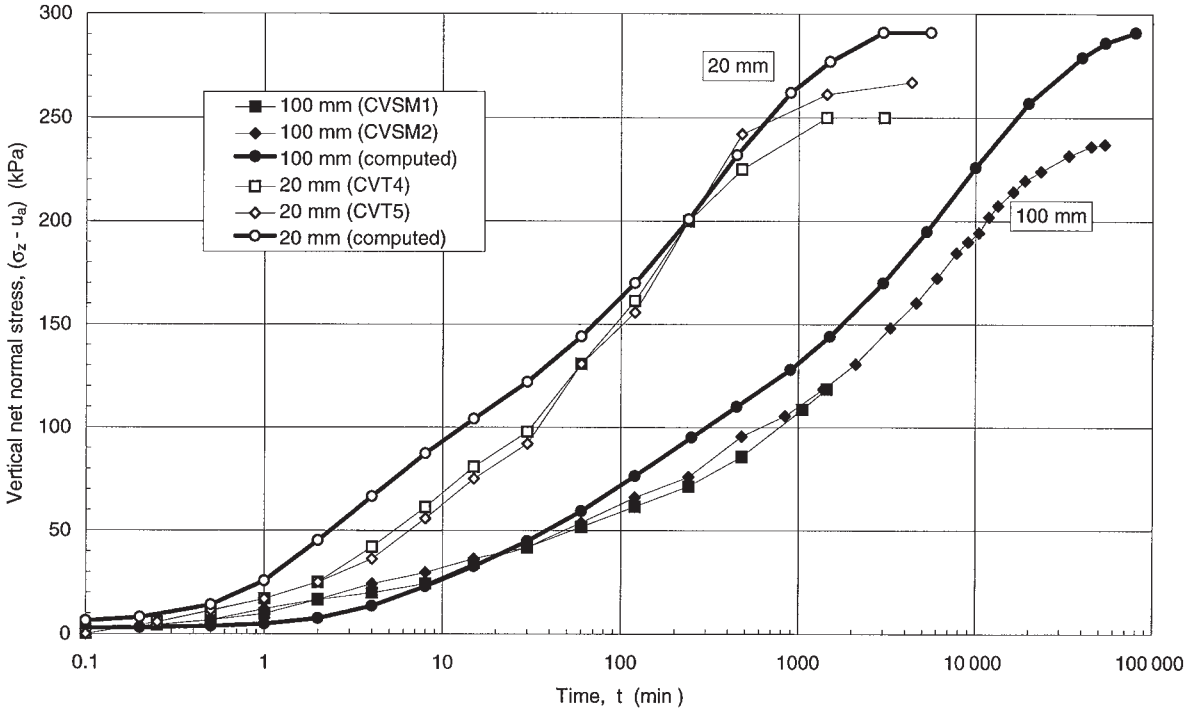

occur when adjusting the applied load. This small swelling could decrease the measured vertical stress. This assumption is supported by the fact that this overestimation does not occur for the 100 mm high specimens.

The measured and computed profiles of matric suction are presented in Fig. 18. The correlations between the measured and computed matric suctions are good. The computed vertical strain profiles are presented in Fig. 19. It should be noted that, during the early stage of the test, the soil on the lower part of the specimen expanded while the soil in the upper part was subjected to compression. With time, the expanding portion of the specimen increased while the net expansion for the wetted segment decreased. In other words, the soil in the zone which originally swelled was subjected to compression under increasing applied load. Additional evidence that can be used to support this deduction is that the rate of vertical pressure development decreased with an increasing height of specimen. As mentioned previously, the rate of swelling for free-swell oedometer tests is essentially independent of the height of the specimen. Therefore, if there were no compressive zone in the upper part of the specimen to partially compensate for the expansion in the lower part, the rate of vertical pressure development would be independent of the height of the specimen. Since there is more space for a high specimen to compensate for the swelling developed in the lower part of the specimen than for a short specimen, the rate of vertical pressure development for a high specimen is much lower than that for a short specimen. Similar vertical strain profiles for the constant-volume test were reported by Alonso et al. (1987).

For a proper interpretation of this phenomenon, it is necessary to study the entire testing process. During the early stages of the constant-volume oedometer test, the soil at the lower part of the specimen begins to wet and tends to expand. However, the soil in the upper part of the specimen does not get water so it did not tend to expand. To keep the overall volume change of the specimen equal to zero, a load is applied to the top of the specimen. Under this load, the soil on the top of the specimen is compressed, but this load is not large enough to prevent the soil in the lower part from expanding. Therefore, during the early stages of the test, the soil in the lower part of the specimen expands while the soil in the upper part compresses. The expanding volume in the lower part of the specimen must be equal to the compressed volume in the upper part. With time, the swelling zone in the specimen increases due to the advance of the wetting front while the volume change in the swelling zone decreases due to increasing applied load and eventually becomes zero at the end of the test.

Loaded-swell oedometer test

Computer simulations of the loaded-swell oedometer testing process were carried out by specifying a zero flux boundary for the top of the specimen and a zero pore-water pressure and zero displacement for the bottom. The initial matric suction and initial void ratio were obtained from the simulation of the constant water content test. The initial stress for all elements was equal to the applied load.

The measured and computed deflection versus time curves are shown in Fig. 20. The computed and measured deflection–time curves show good agreement when the applied load is higher than 300 kPa. Both computed and measured curves indicate a collapse phenomenon when the applied load is higher than 400 kPa. The predicted collapse curve is in a good agreement with the measured laboratory results (Fig. 21). The collapse is due to an increase in the compressibility of the soil which results from a decrease in matric suction.

Both the computed and measured curves demonstrate a double swelling-collapse character when the applied load is equal to 400 kPa (Fig. 22). The specimen swells during the early

Fig. 18. Computed and measured matric suction profiles for constant-volume oedometer test.

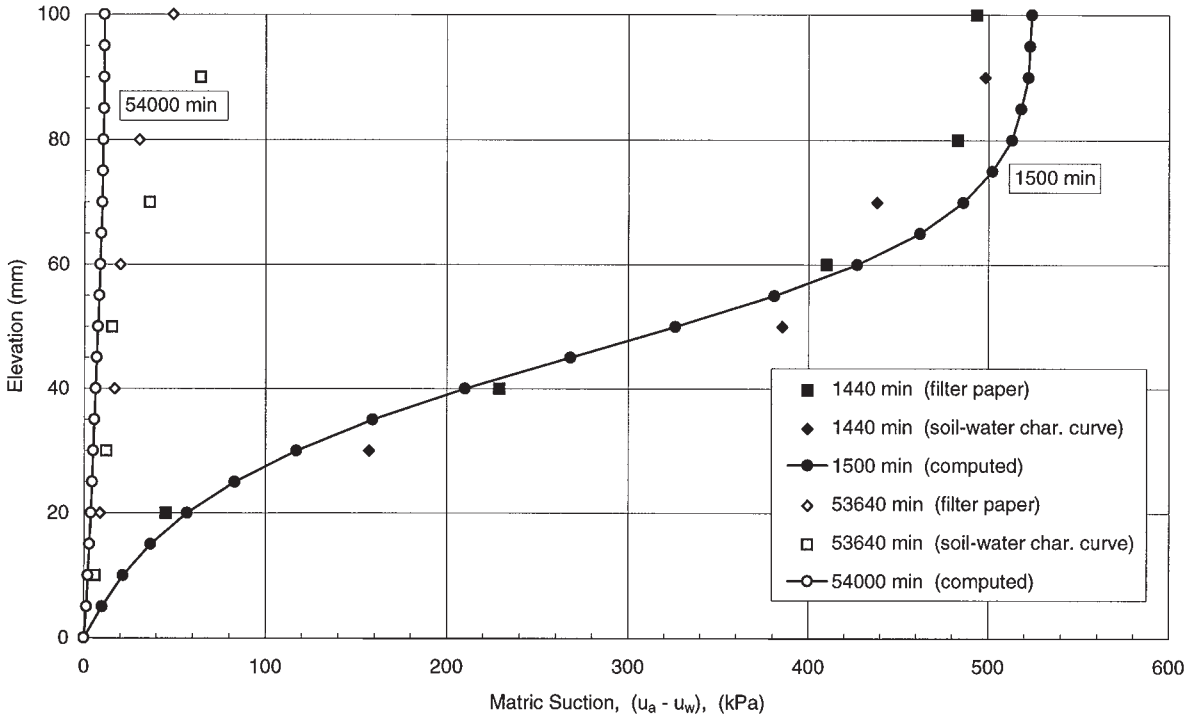

Fig. 19. Computed vertical strain profiles at various times during constant-volume oedometer test.

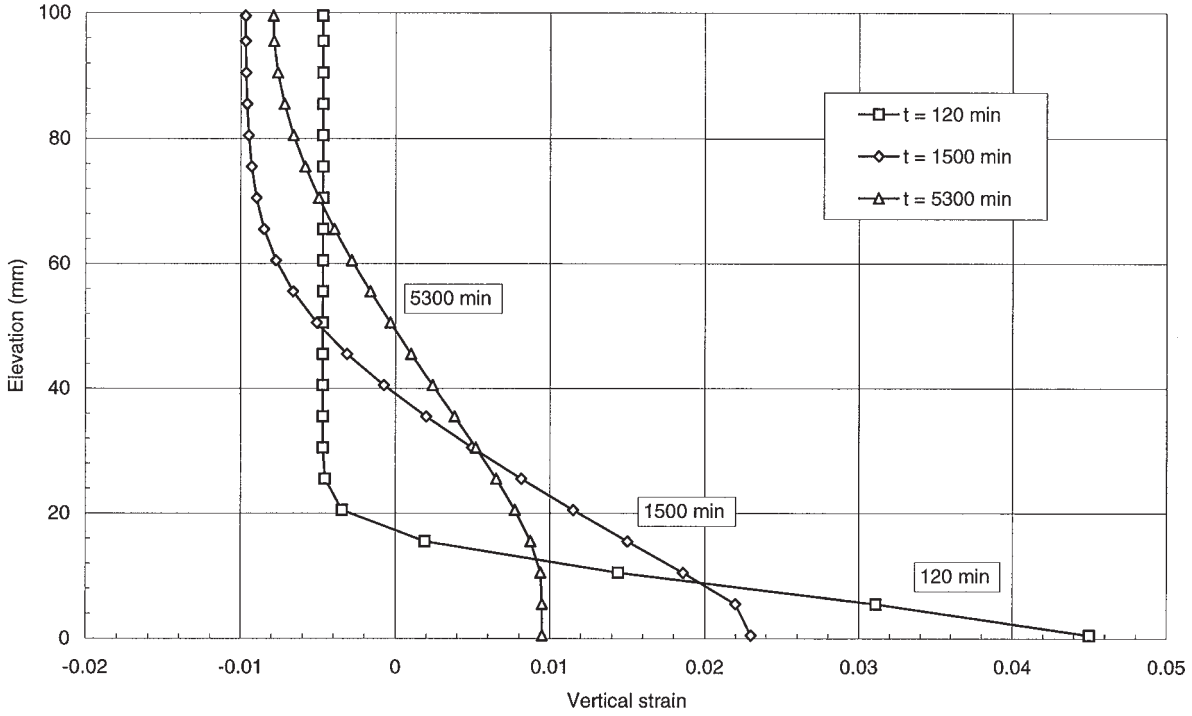

stages of the test, but collapses during the later stages; the magnitude of swell or collapse is quite small. A similar observation was reported by Escario and Saez (1973).

The correlation between the measured and computed deflection–time curves is not as good during the later stages of the test when the applied load is lower than 300 kPa. For example, the measured total heave under an applied load of 100 kPa is 0.543 mm, but is computed to be 1.06 mm. The discrepancy could be attributed to the high ratio of horizontal stress to vertical stress (i.e., σ_h/σ_v) at the end of the test.

Komornik and Zeitlen (1965) used a special oedometer to measure the lateral swelling pressure under different vertical

Fig. 20. Computed and measured deflection versus time relationship for loaded-swell oedometer tests.

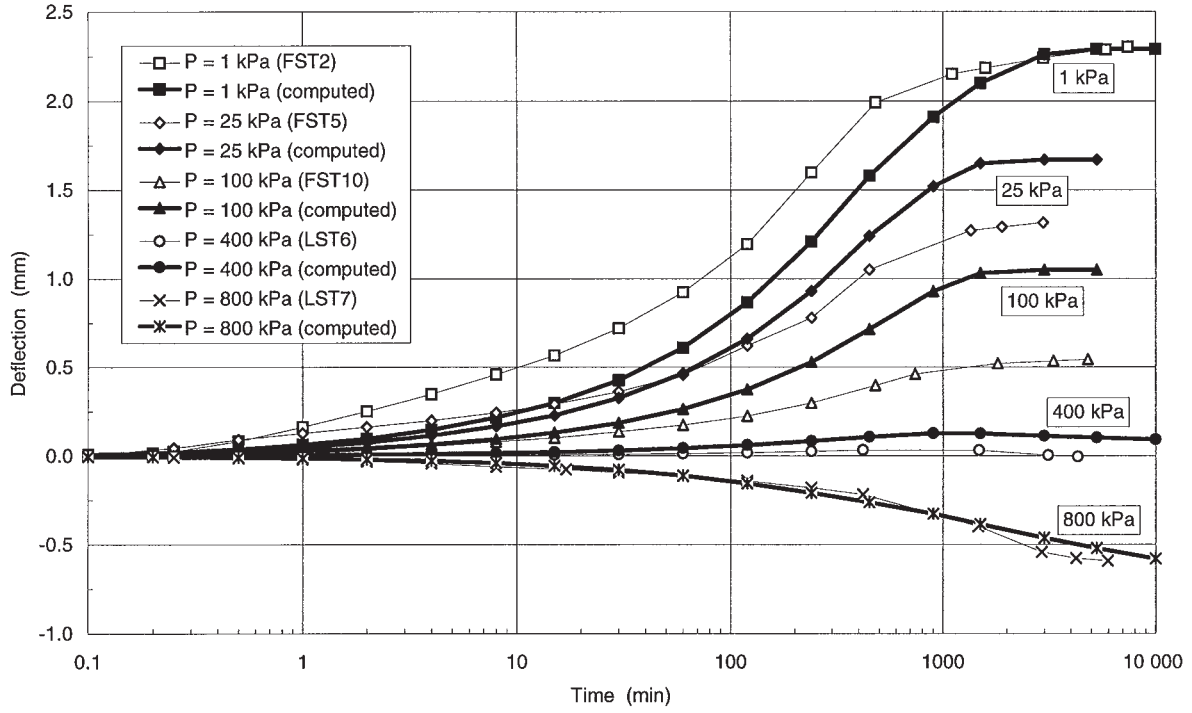

Fig. 21. Computed and measured deflection versus time curves for loaded-swell oedometer test with a load of 800 kPa.

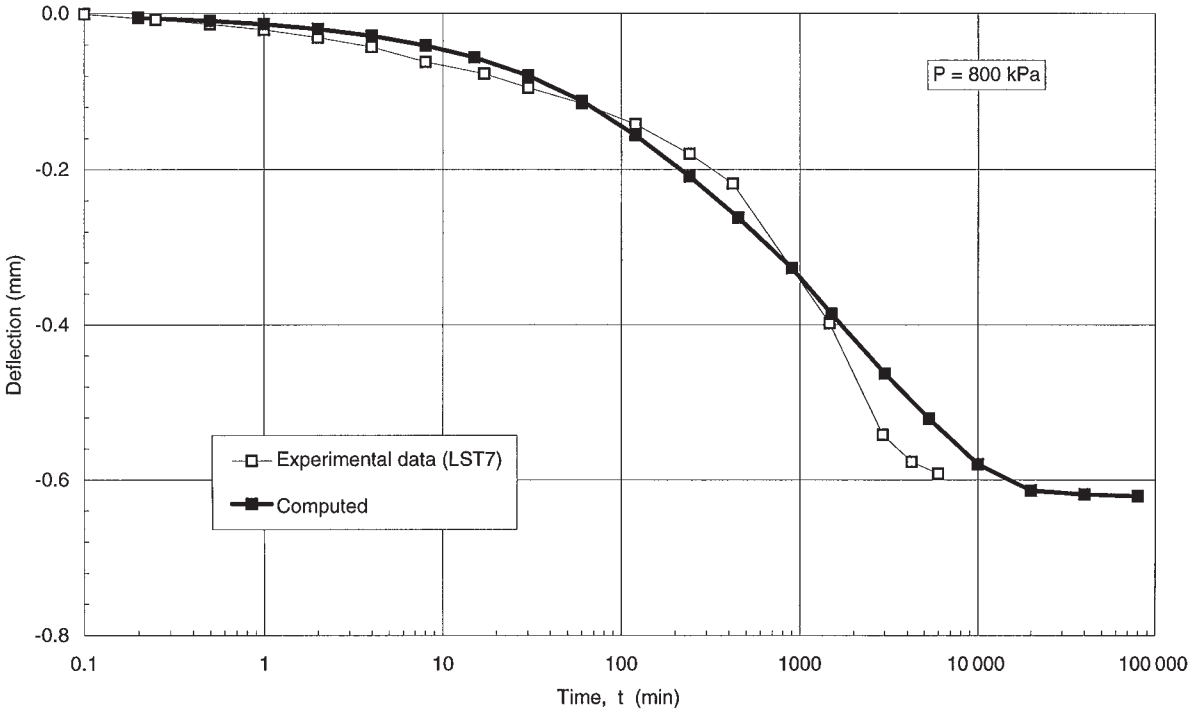

loads. The results obtained indicated that the ratio of horizontal stress to vertical stress at the end of the test increased as the amount of swell increased. In other words, under a constant vertical stress, the mean normal stress applied to the soil increases at the end of the test. The test results obtained by Dakshanamurthy (1979) showed that total heave decreased with increasing mean normal stress. Therefore, the increase in the mean normal stress due to the increasing stress ratio (i.e., σ_h/σ_v) will decrease the total heave at the end of the loaded-swell test. Since the increase in the ratio of horizontal stress to vertical stress has not been taken into account in this theoretical simulation, it should be expected that the calculation results will overestimate the total heave. The amount of the overestimation will decrease as the applied load increases,

Fig. 22. Computed and measured deflection versus time curves for loaded-swell oedometer test with a load of 400 kPa.

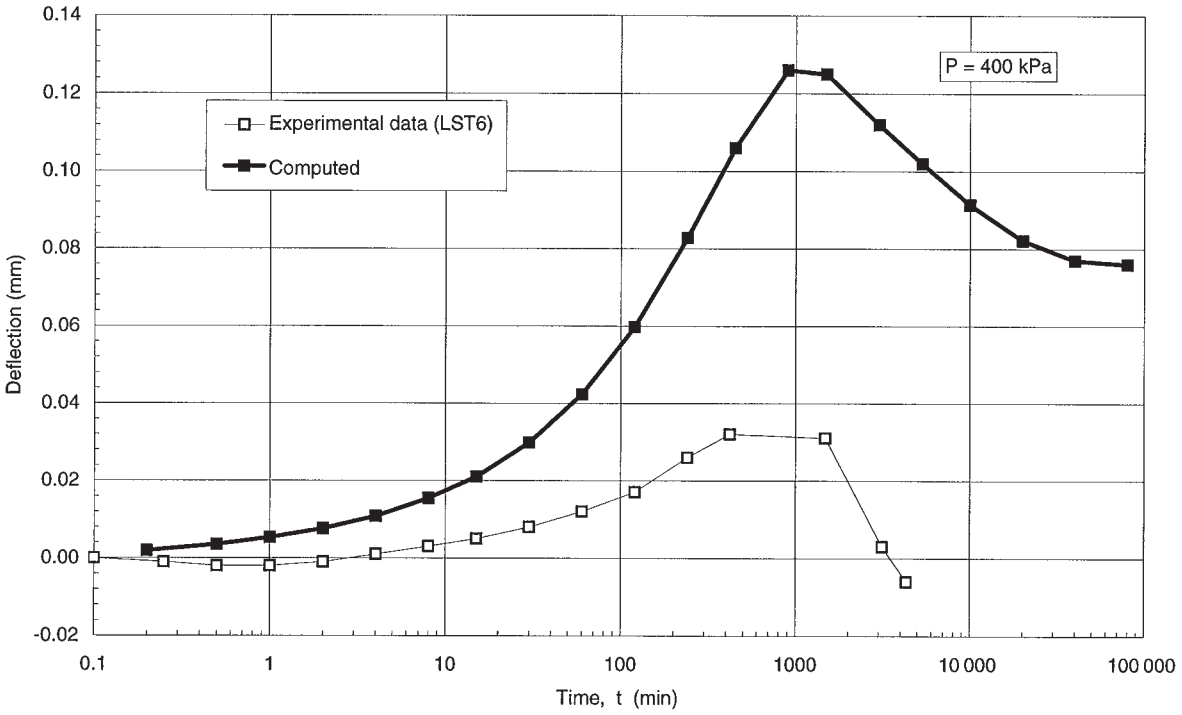

Fig. 23. Computed and measured void ratio versus net normal stress curves for loaded-swell oedometer test.

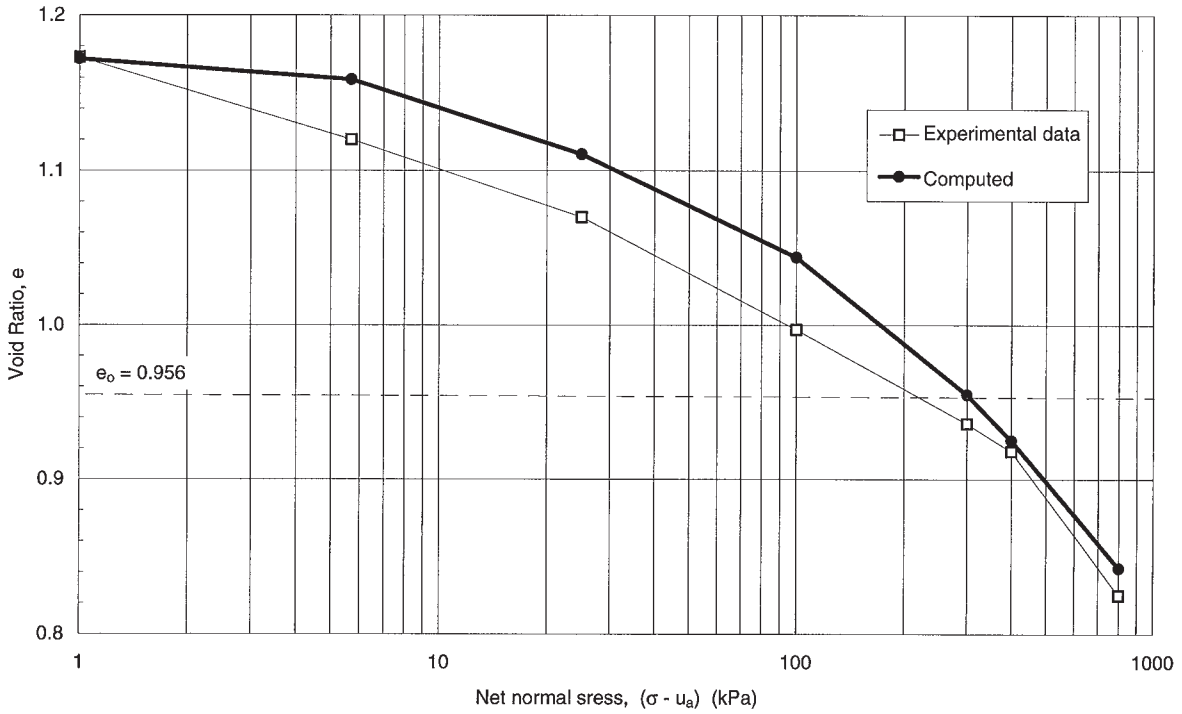

since the ratio of horizontal stress to vertical stress decreases with increasing vertical applied load and decreasing amount of swell.

The measured and computed void ratio versus applied load relationship for the loaded-swell oedometer test is shown in Fig. 23. The intersection of the computed void ratio versus applied load curve with the initial void ratio line (i.e., void ratio equal to 0.960) gives a swelling pressure of 300 kPa, which is close to the corrected swelling pressure (i.e., 300 kPa) and the computed swelling pressure from a simulation of constant-volume test (i.e., 293 kPa) but higher than the measured swelling pressure from the loaded-swell oedometer test (i.e., 210 kPa).

Summary and conclusions

A theoretical model has been formulated to describe the pore-water pressure and volume-change behaviour during various swelling oedometer tests. The model is based on the equilibrium equation, the constitutive equations for unsaturated soils, and the continuity equation for the pore fluids. The transient water flow process is coupled with the soil volume change process in this model. The model can be used to describe the volume-change behaviour, both swelling and collapse, and vertical total stress and pore-water pressure development of an unsaturated soil during an oedometer test.

A finite element formulation has been proposed as a numerical solution for the theoretical model. The computer program SWELL was developed based on the proposed formulation. This program can handle extreme nonlinearities in material properties, varying initial conditions, soil heterogeneity, and arbitrary boundary conditions and external loading conditions.

The following soil properties are required for the theoretical simulations: the coefficient of permeability function (i.e., k_w), the coefficients of soil structure volume change (i.e., m_1^s and m_2^s), and the coefficients of water volume change (i.e., m_1^w and m_2^w). These soil properties can be obtained by performing independent laboratory tests (e.g., saturated permeability tests, free-swell oedometer tests, pressure-plate tests, shrinkage tests, and constant-suction consolidation tests).

The proposed theoretical model was used to simulate the results from free-swell, constant-volume, constant water content (i.e., undrained loading), and loaded-swell oedometer tests. In general, good agreement was found between the computed and measured values of volume change, vertical total stress, pore-water pressure, and swelling pressure. Some overestimation of total heave was noted for loaded-swell oedometer tests when the surcharge loads were significantly lower than the swelling pressure. This poor prediction is attributed to the increasing ratio of horizontal stress to vertical stress at the end of the test which is not possible to simulate using a one-dimensional model. Therefore, a two- or three-dimensional model should be developed on the basis of this model to better understand the volume-change behaviour of expansive soils during a loaded-swell oedometer test.

The work presented in this paper concentrated on a theoretical simulation of the swelling-pressure measurements commonly performed in a laboratory. However, a two- or three-dimensional model can be developed on the basis of this model. This model would greatly assist in the prediction of in situ total heave or collapse, the in situ swelling pressure, and the rate of swell or collapse.

References

Ali, E.F.M., and Elturabi, M.A.D. 1984. Comparison of two methods for the measurement of swelling pressure. *In* Proceedings of the 5th International Conference on Expansive Soils, Adelaide, Australia, pp. 72–74.

Alonso, E.E., Gens, A., and Hight, D.W. 1987. General report: special problem soils. *In* Proceedings of the 9th European Conference on Soil Mechanics and Foundation Engineering, Dublin, Ireland, Vol. 1, pp. 1087–1146.

Bishop, A.W. 1954. The use of pore pressure coefficients in practice. Géotechnique, **4**(4): 148–152.

Brackley, I.J.A. 1975. A model of unsaturated clay structure and its application to swell behavior. *In* Proceedings of the 6th African Regional Conference on Soil Mechanics and Foundation Engineering, Vol. 1, pp. 65–70.

Buckingham, E. 1907. Studies of the movement of soil moisture. U.S. Department of Agriculture, Bureau of Soils, Bulletin No. 38.

Childs, E.C., and Collis-George, N. 1950. The permeability of porous material. Proceedings of the Royal Society of London, A, **201**: 392–405.

Dakshanamurthy, V. 1979. A stress-controlled study of swelling characteristics of compacted expansive clays. Geotechnical Testing Journal, **2**(1): 57–60.

Escario, V., and Saez, J. 1973. Measurement of the properties of swelling and collapsing soil under controlled suction. *In* Proceedings of the International Conference on Expansive Soils, Haifa, Isreal, Vol. 1, pp. 195–200.

Fredlund, D.G. 1979. Second Canadian Geotechnical Colloquium: Appropriate concepts and technology for unsaturated soils. Canadian Geotechnical Journal, **16**(1): 121–139.

Fredlund, D.G. 1981. Seepage in saturated soils, panel discussion: ground water and seepage problem. *In* Proceedings of the 10th International Conference on Soil Mechanics and Foundation Engineering, Stockholm, Sweden, Vol. 4, pp. 629–641.

Fredlund, D.G. 1995. The prediction of heave in expansive soils. *In* Proceedings of the Canada–Kenya Symposium on Unsaturated Soil Behavior and Applications, University of Nairobi, Nairobi, Kenya, pp. 105–119.

Fredlund, D.G., and Rahardjo, H. 1993. Soil mechanics for unsaturated soils. John Wiley & Sons, New York.

Fredlund, D.G., Hasan, J.U., and Filson, H. 1980. The prediction of total heave. *In* Proceedings of the 4th International Conference on Expansive Soils, Denver, Colo., Vol. 1, pp. 1–17.

Freeze, R.A., and Cherry, J.A. 1979. Groundwater. Prentice Hall Inc., Englewood Cliffs, N.J.

Gizienski, S.F., and Lee, L.J. 1965. Comparison of laboratory swell tests to small scale field tests. *In* Proceedings of the 1st International Conference on Expansive Clay Soils. Texas A&M Press, College Station, Tex. pp. 108–119.

Hardy, R.M. 1965. Identification and performance of swelling soil types. Canadian Geotechnical Journal, **2**(2): 141–153.

Holtz, W.G., and Gibbs, H.J. 1956. Engineering properties of expansive clays. Transactions of the American Society of Civil Engineers, **121**: 641–663.

Jennings, J.E., and Knight, K. 1957 The prediction of total heave from the Double Oedometer test. *In* Proceedings of a Symposium on Expansive Clays. South African Institute of Civil Engineers, Johannesburg, South Africa, Vol. 7, No. 9, pp. 13–19.

Jones, D.E., and Holtz, W.G. 1973. Expansive soils–the hidden disaster. *In* Civil engineering. American Society of Civil Engineers, New York. pp. 87–89.

Komornik, A., and Zeitlen, J.G. 1965. An apparatus for measuring lateral soil swelling pressure in the laboratory. *In* Proceedings of the 6th International Conference on Soil Mechanics and Foundation Engineering, Montréal, Que., Vol. 1, pp. 278–281.

Krohn, J.P., and Slosson, J.E. 1980. Assessment of expansive soils in the United States. *In* Proceedings of the 4th International Conference on Expansive Soils, Denver, Colo., Vol. 1, pp. 596–608.

Lambe, T.W., and Whitman, R.V. 1959. The role of effective stress in the behavior of expansive soils. Quarterly of the Colorado School of Mines, **54**(4): 33–60.

Matyas, E.L. 1969. Some properties of two expansive clays from Western Canada. *In* Proceedings of the 2nd International Conference on Expansive Clay Soils. Texas A&M University, College Station, Tex. pp. 263–278.

Noble, C.A. 1966. Swelling measurements and prediction of heave for lacustrine clay. Canadian Geotechnical Journal, **3**(1): 32–41.

Richards, L.A. 1931. Capillary conduction of liquids through porous medium. Journal of Physics, **1**: 318–333.

Shuai, F. 1996. Simulation of swelling pressure measurements on expansive soils. Ph.D. dissertation, University of Saskatchewan, Saskatoon, Sask.

Skempton, A.W. 1954. The pore pressure coefficients, A and B. Géotechnique, **4**(4): 143–147.

Skempton, A.W. 1961. Horizontal stresses in an overconsolidated Eocene clay. *In* Proceedings of the 5th International Conference on Soil Mechanics and Foundation Engineering, Vol. 1, pp. 351–357.

Sridharan, A., Rao, A.S., and Sivapullaiah, P.V. 1986. Swelling pressure of clays. Geotechnical Testing Journal, **9**(1): 24–33.